Synthesis and Reactivity of Bridging Imido and Imido–Oxo Complexes of Iridium. Water-Catalyzed and -Uncatalyzed Dimerization of Terminal Iridium Imido Complexes

Daniel A. Dobbs and Robert G. Bergman*

Department of Chemistry, University of California, Berkeley, California 94720

Received August 3, 1994[⊗]

Bridging imido and imido–oxo complexes having the general structure Cp*Ir(μ-X)(μ-NR)-IrCp* (**1** X = O, R = *tert*-butyl; **3** X = NR, R = Ph; **9** X = NR, R = 2,6-dimethylphenyl; **10** X = O, R = 2,6-dimethylphenyl; **15** X = NR, R = 2,6-dimethyl-4-nitrophenyl; **17** X = NR, R = 2,6-dimethyl-3-nitrophenyl; **18** X = NR, R = 2-methylphenyl) have been prepared. Complex **1** undergoes oxygen transfer to phosphine. Complex **3** undergoes imide transfer to phosphine and reacts with hydrogen. Despite the fact that systems in which both monomers and dimers having the same substituents on the imide moiety are uncommon, monomeric imido complexes of the form Cp*Ir≡NR (**8**, R = 2,6-dimethylphenyl; **11**, R = 2,6-diethylphenyl; **13**, R = 2,6-diisopropylphenyl; **14**, R = 2,6-dimethyl-4-nitrophenyl; **16**, R = 2,6-dimethyl-3-nitrophenyl) have been observed to undergo dimerization. The dimerization of **8** was found to be water-catalyzed and proceeds through intermediate **10**. This reaction is dependent on steric effects and substituent effects. It was found also that dimeric imido complexes **17** and **18** have rigid aryl groups on the imido functionality in solution.

Introduction

Transition-metal imido complexes have received considerable study recently, primarily because they are believed to be intermediates in many important catalytic processes including imide group transfer,[1–6] ammoxidation,[7] and reduction of nitroaromatics.[8] Furthermore, isolable imido complexes have been shown to be reactive toward organic substrates undergoing stoichiometric reactions with, for example, acetylenes, alkenes, carbon monoxide, and ketones.[9–11] Despite the potential for new reactivity, few examples of low-oxidation-state late transition-metal imido complexes have been examined.[12–17]

We earlier reported the synthesis of the first monomeric iridium imido complexes and, in all cases, we observed terminal imido ligands bound to iridium in these complexes.[13] We were interested in whether iridium imido complexes can exist with bridging imido ligands between metal centers, as has been seen in other late-transition-metal imido systems.[11,14–18] We report here the synthesis and reactivity of a series of iridium imido complexes which contain bridging imido ligands.[19] In contrast to the terminal imido complex Cp*Ir≡N-*t*-Bu, one of the bridging imido complexes we have made undergoes imide transfer to phosphine and hydrogenation of the imido moiety. We also report a study of both the water-mediated and thermal dimerization of monomeric iridium imido complexes which contain a 2,6-disubstituted aryl group on the nitrogen atom, including the steric and electronic aspects of this reaction. These reactions are unique in that few examples of monomeric and dimeric imido complexes with the same empirical formula are known in which each species is stable and there is a significant barrier to interconversion.[9] Lastly, we present evidence for hindered rotation of the aryl groups of the dimeric imido complexes in solution.

Results and Discussion

Synthesis and Reactivity of Bridging Imido Complexes. Although imido complexes of iridium contain sterically large imido groups as terminal functionalities,[13] we have found that the same sterically encumbered ligands can bridge two iridium centers. Our first evidence for such bridging imido complexes was obtained by treatment of Cp*Ir≡N-*t*-Bu with 1 equiv of water in THF, which resulted in the loss of *tert*-butylamine and the formation of a new complex, the

[⊗] Abstract published in *Advance ACS Abstracts,* October 1, 1994.

(1) Evans, D. A.; Faul, M. M.; Bilodeau, M. T. *J. Org. Chem.* **1991**, *56*, 6744.
(2) Holm, R. H.; Harlan, E. W. *J. Am. Chem. Soc.* **1990**, *112*, 186.
(3) Williams, G. D.; Whittle, R. R.; Geoffroy, G. L.; Rheingold, A. L. *J. Am. Chem. Soc.* **1987**, *109*, 3936.
(4) Mahy, J.; Battioni, P.; Mansuy, D. *J. Am. Chem. Soc.* **1986**, *108*, 1079.
(5) Svastis, E. W.; Dawson, J. H.; Breslow, R.; Gellman, S. H. *J. Am. Chem. Soc.* **1985**, *107*, 6427.
(6) Breslow, R.; Gellman, S. H. *J. Am. Chem. Soc.* **1983**, *105*, 6728.
(7) Maatta, E. A.; Du, Y. J. *J. Am. Chem. Soc.* **1988**, *110*, 8249–8250 and references therein.
(8) Franck, H. G.; Stadelhofer, J. W. *Industrial Aromatic Chemistry*; Springer-Verlag: Berlin, 1987.
(9) Walsh, P. J.; Hollander, F. J.; Bergman, R. G. *Organometallics* **1993**, *12*, 3705.
(10) Ge, Y.; Sharp, P. R. *Inorg. Chem.* **1992**, *31*, 379.
(11) Han, S.; Geoffroy, G. L. *Organometallics* **1987**, *6*, 2380.
(12) Michelman, R. I.; Bergman, R. G.; Andersen, R. A. *Organometallics* **1993**, *12*, 2741.
(13) Glueck, D. S.; Wu, J.; Hollander, F. J.; Bergman, R. G. *J. Am. Chem. Soc.* **1991**, *113*, 2041.
(14) Ge, Y.; Sharp, P. R. *J. Am. Chem. Soc.* **1990**, *112*, 3667.
(15) Kee, T. P.; Park, L. Y.; Robbins, J.; Schrock, R. R. *J. Chem. Soc., Chem. Commun.* **1991**, 121.
(16) Lee, S. W.; Trogler, W. C. *Inorg. Chem.* **1990**, *29*, 1099.
(17) Nichols, P. J.; Fallon, G. D.; Murray, K. S.; West, B. O. *Inorg. Chem.* **1988**, *27*, 2795.
(18) Abel, E. W.; Blackmore, T.; Whitley, R. J. *Inorg. Nucl. Chem. Lett.* **1974**, *10*, 941.
(19) A portion of this work has been published in an earlier communication: Dobbs, D. A.; Bergman, R. G. *J. Am. Chem. Soc.* **1993**, *9*, 3836.

0276-7333/94/2313-4594$04.50/0

Scheme 1

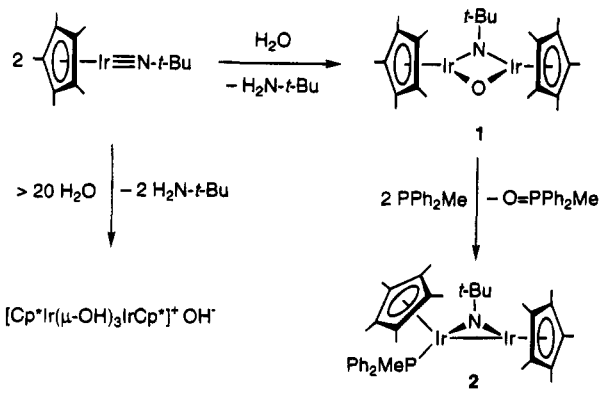

μ-imido, μ-oxo species Cp*Ir(μ-O)(μ-N-*t*-Bu)IrCp* (**1**) (Scheme 1). Complex **1** was isolated in 96% yield as red microcrystals after recrystallization from pentane. Addition of greater than 20 equiv of water to Cp*Ir≡N-*t*-Bu produced the known yellow tris(μ-hydroxide) complex, [Cp*Ir(μ-OH)$_3$IrCp*]$^+$OH$^-$, and *tert*-butylamine (Scheme 1).[20]

The imido–oxo complex **1** was shown to be an oxygen atom transfer agent by reaction with phosphine. Treatment of **1** with 2 equiv of PPh_2Me produced 1 equiv of $O{=}PPh_2Me$ and the bridging imido phosphine complex Cp*Ir(PPh_2Me)(μ-N-*t*-Bu)IrCp* (**2**) (Scheme 1). This oxygen atom transfer reaction is analogous to that observed in the treatment of Cp*Ir(μ-O)$_2$IrCp* with phosphines.[21] An X-ray diffraction study confirmed the structure of complex **2**; an ORTEP diagram is shown in Figure 1. One notable aspect of the structure is a short Ir–Ir distance of 2.694(1) Å, indicating the presence of a metal–metal bond. The short Ir2–N distance of 1.810(10) Å[22] suggests Ir–N multiple bonding between the formally 16-electron Ir2 center and the planar nitrogen atom, as compared to the Ir1–N separation of 1.972(1) Å at the formally 18-electron iridium atom. Crystal and data collection parameters are found in Table 1 and intramolecular distances and angles are contained in Tables 2 and 3.

Although earlier attempts to prepare imido complexes from sterically unencumbered lithium arylamides and [Cp*IrCl$_2$]$_2$ were unsuccessful,[13] such complexes can be prepared by other methods. Treatment of the imido–oxo complex **1** with aniline resulted in the production of the bridging bis(phenylimido) complex Cp*Ir(μ-NPh)$_2$IrCp* (**3**) and the loss of 1 equiv of *tert*-butylamine and water (Scheme 2). Bis(imido) complex **3** also was prepared by the treatment of Cp*Ir≡N-*t*-Bu with aniline. An ORTEP diagram of **3** is shown in Figure 2. The structure displays a short Ir–Ir distance of 2.778(1) Å, indicating some metal–metal interaction. The nitrogen atoms are pyramidal (sum of the angles about each nitrogen is 338°) and the Ir–N distances are 1.986(av) Å. Crystal and data collection parameters are found in Table 1, and intramolecular distances and angles are found in Tables 4 and 5.

The short Ir–Ir distance in dimeric complex **3** is well within the range observed for typical Ir–Ir bonds.

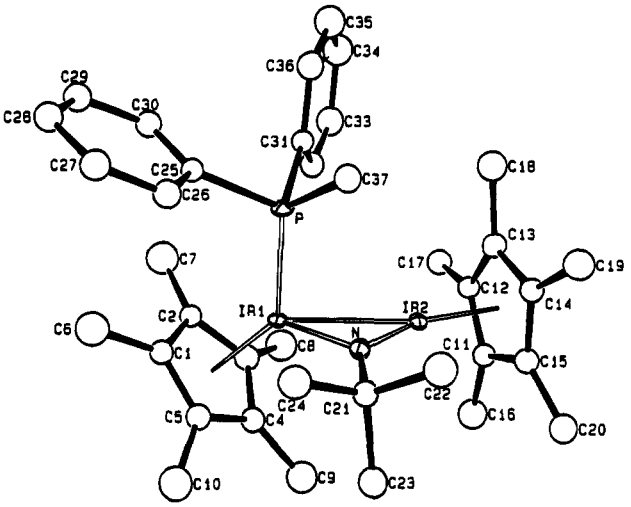

Figure 1. ORTEP diagram of compound **2**. Thermal ellipsoids are at the 50% probability level.

However, the observed puckering of the Ir$_2$N$_2$ core may be the result of second-order Jahn–Teller effects. That is, the bent form may be stabilized relative to the planar form through the lessening of filled–filled d–π interactions between occupied d and π molecular orbitals.[23,24]

Like the terminal imido complexes of iridium,[13] the dimeric imido complex **3** is reactive. Imide transfer to PMe_3 was observed upon heating **3** with 2 equiv of PMe_3 at 85 °C, forming the phosphinimine $PhN{=}PMe_3$ and Cp*Ir(PMe_3)(μ-NPh)IrCp* (**4**), a complex analogous to the monobridged imido complex **2** (Scheme 3). Complex **4** was characterized by analytical and spectroscopic techniques including FAB mass spectrometry. The mass spectrum of **4** displayed a peak for a protonated molecular ion at *m/e* 820. The phosphinimine $PhN{=}PMe_3$ was prepared independently by the addition of phenyl azide to PMe_3[25] and compared by ^{1}H, ^{13}C{^{1}H}, and ^{31}P{^{1}H} NMR spectroscopy and mass spectrometry to the phosphine compound produced from the reaction of **3** and PMe_3.

An intermediate was observed by ^{1}H NMR spectroscopy during the course of the imide transfer reaction (after 1 h at room temperature). This complex could not be isolated, but it is formulated by ^{1}H and ^{31}P{^{1}H} NMR spectroscopy as the PMe_3 adduct of the bis(imido) complex **3**, Cp*Ir(PMe_3)(μ-NPh)$_2$IrCp* (**5**) (Scheme 3). Therefore, we propose that the imide transfer reaction proceeds through initial attack on the imido complex **3** by PMe_3 to form **5** followed by imide transfer, loss of the phosphinimine, and finally, coordination of free PMe_3.

The addition of phosphine to dimeric imide **3** in the presence of water changed the observed reactivity. Treatment of imido complex **3** with 1 equiv of water and 2 equiv of PMe_3 at room temperature resulted in the formation of mono(imido) complex **4**, 1 equiv of $O{=}PMe_3$, and 1 equiv of aniline. Moreover, addition of water to bridging imido complex **3** in the absence of PMe_3 produced no change in the spectral characteristics of **3**. Our rationalization for these observations is that water reacts reversibly with the bis(imido) complex **3** to

(20) Nutton, A.; Bailey, P. M.; Maitlis, P. M. *J. Chem. Soc., Dalton Trans.* **1981**, 1997.
(21) McGhee, W. D.; Foo, T.; Hollander, F. J.; Bergman, R. G. *J. Am. Chem. Soc.* **1988**, *110*, 8543.
(22) Baranger, A. M.; Hollander, F. J.; Bergman, R. G. *J. Am. Chem. Soc.* **1993**, *115*, 7890.
(23) Kee, T. P.; Park, L. Y.; Robbins, J.; Schrock, R. R. *J. Chem. Soc., Chem. Commun.* **1991**, 121.
(24) Loren, S. D.; Campion, B. K.; Heyn, R. H.; Tilley, T. D.; Bursten, B. E.; Luth, K. W. *J. Am. Chem. Soc.* **1989**, *111*, 4712.
(25) Franz, J. E.; Osuch, C. *Tetrahedron Lett.* **1963**, 841.

Table 1. Crystal and Data Collection Parameters[a]

compd	2	3	7
temp (°C)	−94	−94	−101
emp formula	$Ir_2PNC_{37}H_{52}$	$Ir_2N_2C_{32}H_{40}$	$Ir_2NC_{26}H_{37}$
fw	926.2	837.1	748.0
cryst size (mm)	0.16 × 0.28 × 0.32	0.27 × 0.31 × 0.48	0.15 × 0.28 × 0.40
space group	$P\bar{1}$	*Pnnm*	$P\bar{1}$
a (Å)	10.726(2)	11.993(3)	9.100(2)
b (Å)	10.742(3)	15.159(4)	10.287(2)
c (Å)	17.248(2)	15.919(5)	13.978(2)
α (deg)	75.476(16)	90.0	75.636(15)
β (deg)	85.824(14)	90.0	78.120(16)
γ(deg)	63.98(2)	90.0	74.212(4)
V (Å^3)	1727.2(5)	2893.9(23)	1206.2(4)
Z	2	4	2
d_{calc} (g cm^{-3})	1.78	1.92	2.06
μ (cm^{-1})	77.4	91.8	109.9
rflns measd	$+h,\pm k,\pm l$	$+h,+k,+l$	$\pm h,\pm k,\pm l$
scan width ($\Delta\theta$)	0.80 + 0.35 tan θ	0.85 + 0.35 tan θ	0.80 + 0.35 tan θ
scan speed (θ, deg/m)	5.49	5.49	8.24
setting angles (2θ, deg)[b]	26−30	26−28	26−30
2θ range (deg)	3−50	3−48	3−50
horiz aperture (mm)	2.2 + 1.0 tan θ	2.2 + 1.0 tan θ	2.0 + 1.0 tan θ
no of rlfns collcd	6074	2428	8444
no. of unique rflns	6074	2282	4351
no. of obs rflns ($F^2 > 3\sigma F^2$)	4685	1763	3204
T_{max}/T_{min}	0.999/0.816	0.999/0.678	1.29/0.84
no. of params refined	180	85	275
$R(F)$ (%)	4.8	4.0	1.89
$R_w(F)$ (%)	6.1	4.6	2.15
R_{all} (%)	6.7	5.9	3.53
goodness of fit	2.43	1.73	0.82

[a] Parameters common to all structures: radiation, Mo Kα (λ = 0.710 73 Å); monochromator, highly-oriented graphite (2θ = 12.2°); detector, crystal scintillation counter, with PHA; vertical aperture = 4.0 mm; scan type, θ−2θ; background, measured over 0.25($\Delta\theta$) added to each end of the scan; intensity standards, measured every hour of X-ray exposure time; orientation, three reflections were checked after every 200 measurements. [b] Unit cell parameters and their esd's were derived by a least-squares fit to the setting angles of the unresolved Mo Kα components of 24 reflections with the given 2θ range. In this and all subsequent tables the esd's of all parameters are given in parentheses, right-justified to the least significant digit(s) of the reported value.

Table 2. Selected Intramolecular Distances (Å) for 2

Ir1−Ir2	2.694(1)	Ir2−N	1.810(10)
Ir1−P	2.208(3)	Ir2−Cp2	1.860(1)
Ir1−N	2.031(10)	N−C21	1.490(17)
Ir1−Cp1	1.918(1)		

Table 3. Selected Intramolecular Angles (deg) for 2

Ir2−Ir1−P	88.43(9)	Ir1−Ir2−N	48.9(3)
Ir2−Ir1−N	42.2(3)	Ir1−Ir2−Cp2	153.37(3)
Ir2−Ir1−Cp1	131.58(2)	N−Ir2−Cp2	157.6(3)
P−Ir1−N	90.3(3)	Ir1−N−Ir2	88.9(4)
P−Ir1−Cp1	133.90(9)	Ir1−N−C21	133.5(8)
N−Ir1−Cp1	133.6(3)	Ir2−N−C21	136.6(9)

Scheme 2

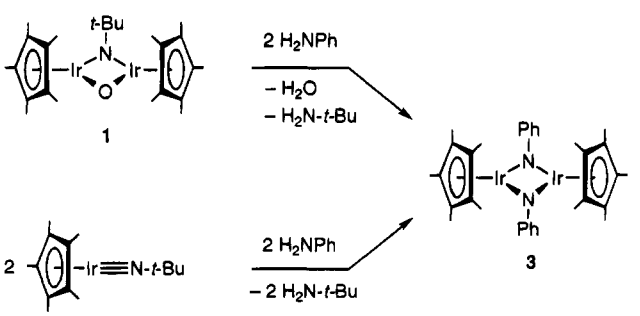

produce Cp*Ir(μ-O)(μ-NPh)IrCp* (**6**) and aniline and that K_{eq} for this reaction is less than unity (Scheme 3). Imido−oxo complex **6** then transfer an oxygen atom to phosphine to produce **4** faster than imide **3** or itself (complex **6**) can transfer an imide moiety.[26,27] An alternate possibility is that the reaction proceeds as before, except that water reacts with PhN=PMe$_3$ to form O=PMe$_3$. We believe this is unlikely because the rate of the reaction is much faster in the presence of water,

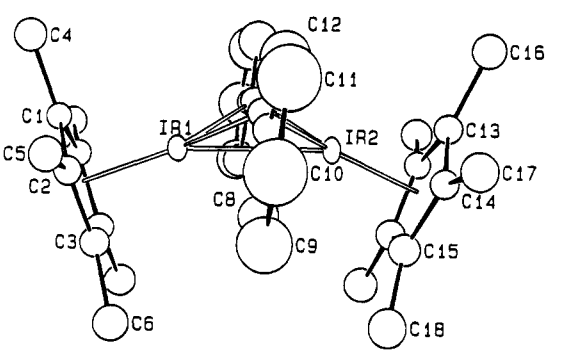

Figure 2. ORTEP diagram of compound **3**. Thermal ellipsoids are at the 50% probability level.

Table 4. Selected Intramolecular Distances (Å) for 3

Ir1−Ir2	2.778(1)	Ir2−N	1.977(10)
Ir1−N	1.994(10)	Ir2−Cp2	1.806
Ir1−Cp1	1.817	N−C7	1.397(15)

Table 5. Selected Intramolecular Angles (deg) for 3

Ir2−Ir1−Cp1	160.1	Ir1−Ir2−N	45.9(3)
N−Ir1−Cp1	142.1	N−Ir2−N	75.1(6)
Ir1−Ir2−N	45.9(3)	Ir1−N−Ir2	88.8(4)
N−Ir1−N	74.3(6)	Ir1−N−C7	125.0(8)
Ir1−Ir2−Cp2	156.2	Ir2−N−C7	124.1(8)
N−Ir2−Cp2	142.2		

and the reaction without water involves a slower step to form the intermediate **5**.

Complex **3** also reacts with hydrogen. Heating **3** under 2 atms of H_2 at 85 °C resulted in the loss of

(26) Oxo transfer has been shown to be faster than imido transfer in at least one other system; see ref 2.
(27) Holm, R. H. *Chem. Rev.* **1987**, *87*, 1401.

Scheme 3

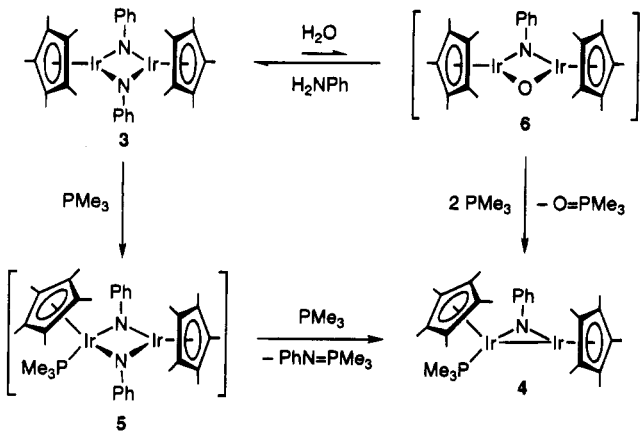

Scheme 4

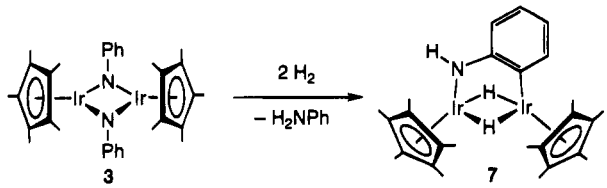

aniline and the formation of a bridging dihydride complex Cp*Ir(μ-NH(*o*-C_6H_4))(μ-H)$_2$IrCp* (**7**) (Scheme 4). This complex is the apparent result of hydrogenation of an imide linkage to form aniline followed by intramolecular C–H activation. Reduction of an imide moiety has been observed only rarely.[28–32] The existence of hydride ligands in this complex was confirmed by ^{1}H NMR spectroscopy, which revealed a resonance at −16.8 ppm. An X-ray structure revealed the salient features of complex **7**. The ORTEP diagram is shown in Figure 3. The hydride ligands were located and occupy symmetrical bridging positions. The complex has a pseudomirror plane, and the nitrogen moiety is planar. Crystal and data collection parameters are found in Table 1, and representative intramolecular distances and angles are listed in Tables 6 and 7.

Conversion of Monomeric Imido Complexes to Dimers: Water-Catalyzed Dimerization. Oxo and imido complexes typically exist as monomers or dimers. Examples of systems in which both monomers and dimers, having identical substituents, can be prepared and directly compared are rare. In our earlier study of imido complexes of iridium, we observed only monomeric complexes.[13] However, we now have found some arylimido complexes that can be prepared as monomers, but can also be converted to dimers, and in these cases the dimeric form is thermodynamically favored. For example, heating Cp*Ir≡N(2,6-dimethylphenyl) (**8**) at 45 °C resulted in the formation dimeric imido complex Cp*Ir(μ-N(2,6-dimethylphenyl))$_2$IrCp* (**9**). The binuclear structure of complex **9** was confirmed by an X-ray crystallographic study, and an ORTEP diagram is shown in Figure 4. Crystal and data collection parameters for complex **9** are found in Table 8, and intramolecular distances and angles are listed in Tables 9 and 10.

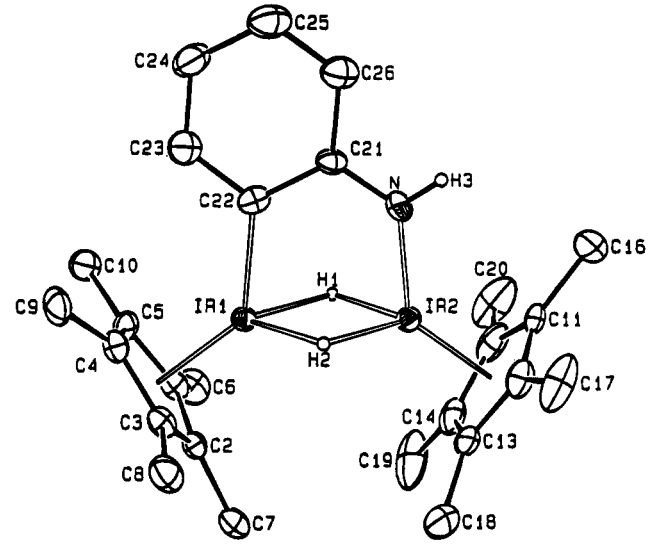

Figure 3. ORTEP diagram of compound **7**. Thermal allipsoids are at the 50% probability level.

Table 6. Selected Intramolecular Distances (Å) for 7

Ir1–Ir2	2.753(1)	Ir1–Cp1	1.853
Ir1–C22	2.032(6)	Ir2–Cp2	1.799
Ir2–N	1.959(5)	N–H3	0.81(6)
Ir–H(avg)	1.88[13]	N–C21	1.362(8)

Table 7. Selected Intramolecular Angles (deg) for 7

Cp1–Ir1–Ir2	142.94	Cp2–Ir2–H2	128.3
Cp1–Ir1–C22	131.30	N–Ir2–Ir1	83.62(16)
Cp1–Ir1–H1	133.1	N–Ir2–H1	81.7(27)
Cp1–Ir1–H2	122.5	N–Ir2–H2	85.3(21)
C22–Ir1–Ir2	85.76(16)	H1–Ir2–H2	83.7(34)
C22–Ir1–H1	82.3(24)	Ir1–H1–Ir2	101.1(39)
C22–Ir1–H2	88.4(24)	Ir1–H2–Ir2	91.8(31)
H1–Ir1–H2	83.1(33)	Ir2–N–C21	129.2(4)
Cp2–Ir2–Ir1	144.75	Ir2–N–H3	117.6(43)
Cp2–Ir2–N	131.62	C21–N–H3	113.0(43)
Cp2–Ir2–H1	129.2		

Comparison of this structure with the analogous bis(phenylimido) dimer **3** revealed some striking differences. Whereas in the phenylimido bridged complex **3** the nitrogen atoms were found to be pyramidal (sum of angles about each nitrogen is 338°), in the structure of 2,6-dimethylphenylimido complex **9** the nitrogen geometry is almost planar (sum of the angles about each nitrogen is 354°). We believe that this structural difference is most likely the result of steric repulsion between the aryl methyl groups and the pentamethylcyclopentadienyl ligands, which forces the nitrogen atoms toward planarity. An alternate explanation is that π-donation from the nitrogen atoms to iridium in the case of the (2,6-dimethylphenyl)imido complex **9** leads to some differential stabilization of this complex. If this were the case, however, the Ir–N distances should be shorter relative to that found in **3**, but this is not observed. The Ir–Ir distance in **9** (2.894(1) Å) is significantly longer than that found in complex **3** (Ir–Ir distance 2.778(1) Å), and we believe that steric effects are most likely responsible for this observed difference.

Because of the lack of isolable monomeric imido complexes which undergo simple dimerization reactions (especially ones that are uncomplicated by dative ligand

(28) Cummins, C. C.; Baxter, S. M.; Wolczanski, P. T. *J. Am. Chem. Soc.* **1988**, *110*, 8731.
(29) Fryzuk, M. D.; MacNeil, P. A.; Rettig, S. J. *J. Am. Chem. Soc.* **1987**, *109*, 2803.
(30) Cowan, R. L.; Trogler, W. C. *Organometallics* **1987**, *6*, 2451.
(31) McKenna, S. T.; Andersen, R. A.; Muetterties, E. L. *Organometallics* **1986**, *5*, 2233.
(32) Bryndza, H. E.; Fong, L. K.; Paciello, R. A.; Tam, W.; Bercaw, J. E. *J. Am. Chem. Soc.* **1987**, *109*, 1444.

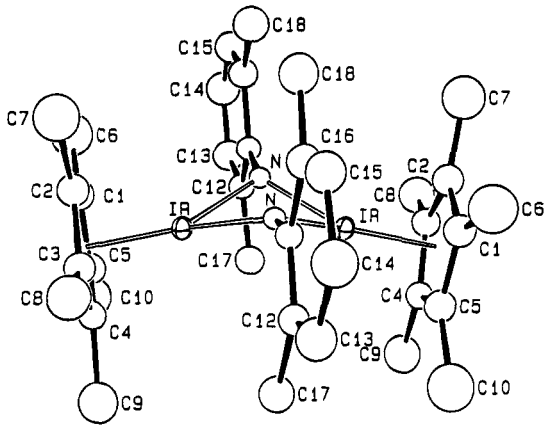

Figure 4. ORTEP diagram of compound **9**. Thermal ellipsoids are at the 50% probability level.

Table 8. Crystal and Data Collection Parameters[a]

compd	**9**	**10**
temp (°C)	−102	−98
emp formula	$IrNC_{18}H_{24}$[c]	$Ir_2ONC_{28}H_{39}$
fw	446.6	790.0
cryst size (mm)	0.17 × 0.27 × 0.30	0.14 × 0.14 × 0.40
space group	*C2/c*	$P2_1/n$
a (Å)	19.197(2)	11.388(2)
b (Å)	8.6800(9)	16.865(2)
c (Å)	21.647(3)	13.695(2)
α (deg)	90.0	90.0
β (deg)	114.900(11)	95.064(13)
γ (deg)	90.0	90.0
V (Å^3)	3271.7(14)	2620.1(13)
Z	8	4
d_{calc} (g cm^{-3})	1.81	2.00
μ (cm^{-1})	81.2	101.3
reflns measd	$+h,+k,\pm l$	$+h,+k,\pm l$
scan width ($\Delta\theta$)	0.70 + 0.35 tan θ	0.65 + 0.35 tan θ
scan speed (θ, deg/m)	5.49	5.49
setting angles (2θ,deg)[b]	26−34	28−30
2θ range (deg)	3−50	3−46
horiz aperture (mm)	2.0 + 1.0 tan θ	2.0 + 1.0 tan θ
no. of reflns collcd	3169	3791
no. of unique rflns	2879	3639
no. of obs rflns ($F^2 > 3\sigma F^2$)	2354	2889
T_{max}/T_{min}	1.000/0.592	0.997/0.594
no. of params refined	86	139
$R(F)$ (%)	3.8	4.0
$R_w(F)$ (%)	4.8	4.6
R_{all} (%)	5.0	5.6
goodness of fit	2.01	1.77

[a] Parameters common to all structures: radiation, Mo Kα (λ = 0.710 73 Å); monochromator, highly-oriented graphite (2θ = 12.2°); detector, crystal scintillation counter, with PHA; vertical aperture = 4.0 mm; scan type, $\theta-2\theta$; background, measured over 0.25($\Delta\theta$) added to each end of the scan; intensity standards, mesaured every hour of X-ray exposure time; orientation, three reflections were checked after every 200 measurements. [b] Unit cell parameters and their esd's were derived by a least-squares fit to the setting angles of the unresolved Mo Kα components of 24 reflections with the given 2θ range. In this and all subsequent tables the esd's of all parameters are given in parentheses, right-justified to the least significant digit(s) of the reported value. [c] This formula corresponds to $^1/_2$ dimer.

Table 9. Selected Intramolecular Distances (Å) for 9

Ir−Ir	2.894(1)	Ir−N′	1.973(7)
Ir−N	1.973(7)	Ir−Cp	1.803

dissociation or other pre−equilibrium reaction steps), we decided to carry out an in-depth examination of the conversion of monomer **8** to dimer **9**.[9,33] This reaction turned out to be somewhat more complicated than we

(33) Arney, D. J.; Bruck, M. A.; Huber, S. R.; Wigley, D. E. *Inorg. Chem.* **1992**, *31*, 3749.

Table 10. Selected Intramolecular Angles (deg) for 9

N−Ir−N′	75.2(4)	Ir−N−Ir	94.4(3)
N−Ir−Cp	141.6	Ir−N−C11	126.8(6)
N′−Ir−Cp	140.6	Ir−N−C11	133.0(6)

Scheme 5

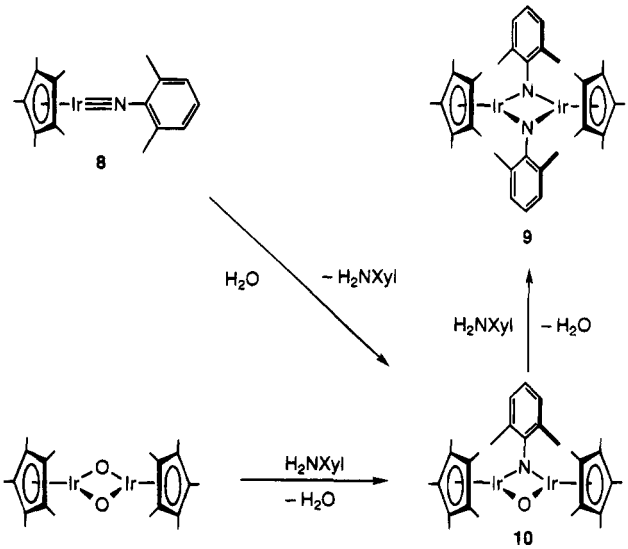

anticipated. The rate of the dimerization reaction of monomeric imido complex **8** was found to be erratic, and it proceeded more rapidly upon addition of small quantities of water. Monitoring the reaction of **8** and water by NMR spectroscopy showed that addition of 1 equiv of water to complex **8** resulted initially in the formation of 2,6-dimethylaniline and an intermediate formulated as a bridging imido−oxo species, Cp*Ir(μ-N(2,6-dimethylphenyl))(μ-O)IrCp* (**10**) (Scheme 5). This reaction is directly analogous to that producing imido−oxo complex **1** (*vide supra*), but in contrast, complex **10** is not stable to the reaction conditions and reacts with the 2,6-dimethylaniline liberated to form the dimeric imido complex Cp*Ir(μ-N(2,6-dimethylphenyl))$_2$IrCp* (**9**).

The reactive μ-oxo, μ-imido complex **10** initially produced from the reaction of **8** and water can be prepared by an independent method. Treatment of Cp*Ir(μ-O)$_2$IrCp*[21] with 0.8 equiv of 2,6-dimethylaniline resulted in the formation of 1 equiv of water and Cp*Ir(μ-N(2,6-dimethylphenyl))(μ-O)IrCp* (**10**) in 28% yield. The structure of this complex was confirmed by an X-ray crystallographic study; an ORTEP diagram is shown in Figure 5. Crystal and data collection parameters are found in Table 8, and representative intramolecular distances and angles are in Tables 11 and 12. Notable aspects of the structure include a short Ir—Ir distance of 2.694(1) Å and a relatively planar nitrogen atom (the sum of the angles around nitrogen is 355°). During the course of these experiments we substantially improved the synthesis of the bridging oxo dimer Cp*Ir(μ-O)$_2$IrCp*. By subjecting the crude product to high vacuum and then lyophilizing it with benzene, the isolated yield can be increased from about 20% to 65%. The revised procedure is included in the Experimental Section.

Conversion of Monomeric Imido Complexes to Dimers: Thermal Dimerization and Kinetic Studies. Having identified the water-catalyzed process discussed above, we sought to ascertain whether the

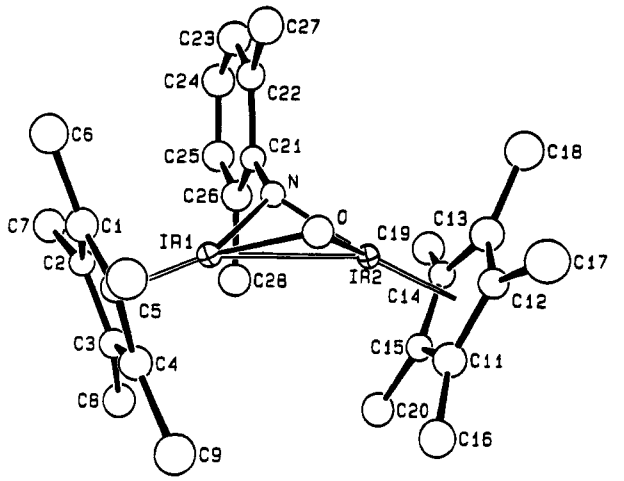

Figure 5. ORTEP diagram of compound **10**. Thermal ellipsoids are at the 50% probability level.

dimerization of the arylimido complex Cp*Ir≡N(2,6-dimethylphenyl) (**8**) can proceed thermally in the absence of water. This is not a straightforward problem because, in general, it is difficult to eliminate all traces of water from a reaction mixture. Most drying reagents are not practical for addition to a reaction solution, in that such substances are often not compatible with the reaction under study, and there is no direct method for ensuring that all the water has been eliminated. We therefore sought a drying agent that reacts completely and irreversibly with water to give an NMR-observable product, that is soluble, and that is stable to the reaction conditions. We decided to use Cp_2ZrMe_2 which is stable to our reaction conditions and is known to react rapidly and irreversibly with water to produce $Cp_2Zr(Me)(\mu\text{-}O)Zr(Me)Cp_2$.[34] Addition of Cp_2ZrMe_2 to solutions of monomeric imido complex **8** initially resulted in the production of a small quantity of $Cp_2Zr(Me)(\mu\text{-}O)Zr(Me)Cp_2$ at room temperature, due presumably to its reaction with the final traces of water in solution. After this initial reaction, the concentration of Cp_2ZrMe_2 and the (μ-oxo)zirconium complex did not change. Heating these solutions of monomer **8** in the presence of Cp_2ZrMe_2 resulted in formation of the dimeric complex **9** (Scheme 6). This reaction required temperatures higher than that required in the presence of water, and no evidence for the production of μ-imido, μ-oxo intermediate **10** was observed by ^1H NMR spectroscopy. Heating complex **8** at 110 °C and monitoring the loss of starting material by ^1H NMR spectroscopy gave linear plots of $[\mathbf{8}]^{-1}$ versus time, indicating second-order behavior ($k_{obs} = 2.5 \times 10^{-2}$ M^{-1} s^{-1}). Varying the concentration of Cp_2ZrMe_2 produced no change in the observed rate of reaction. We believe that this rules out the possibility that either water or Cp_2ZrMe_2 is a catalyst for this reaction. These observations provide good evidence that monomeric imido complex **8** can undergo a simple uncatalyzed bimolecular dimerization.

In order to examine the scope of the dimerization and investigate whether steric effects play a significant role, several complexes with hindered arylimido groups were prepared and heated in the presence of Cp_2ZrMe_2. Heating the 2,6-diethylphenyl analogue of complex **8**, Cp*Ir≡N(2,6-diethylphenyl) (**11**),[35] at 110 °C in the presence of Cp_2ZrMe_2 resulted in the formation of the dimeric complex Cp*Ir(μ-N(2,6-diethylphenyl))$_2$IrCp* (**12**) (Scheme 6). Similar to the reaction of (2,6-dimethylphenyl)imido complex **8**, the addition of Cp_2ZrMe_2 to solutions of monomeric imido complex **11** initially resulted in the production of a small quantity of $Cp_2Zr(Me)(\mu\text{-}O)Zr(Me)Cp_2$ at room temperature, and the concentration of this complex did not change. Monitoring this reaction by ^1H NMR spectroscopy and plotting $[\mathbf{11}]^{-1}$ versus time at early reaction times[36] gave $k_{obs} = 5.8 \times 10^{-4}$ M^{-1} s^{-1}. Therefore, this reaction is significantly slower than that observed for the (2,6-dimethylphenyl)imido complex **8** (k_{obs} (**8**)/k_{obs} (**11**) = 42). The dimeric complex **12** was synthesized independently by heating a mixture of 2,6-diethylaniline and Cp*Ir≡N-*t*-Bu in wet toluene at 75 °C for 3 days (67% yield). The formulation of this complex as a dimer was supported by mass spectrometry and by its similarity in properties to the crystallographically characterized dimeric complex **9**.[37]

In contrast to the 2,6-dimethylphenyl and 2,6-diethylphenyl complexes **8** and **11**, dimerization of the (2,6-diisopropylphenyl)imido complex **13** was not observed. Heating this complex to 200 °C in the presence Cp_2ZrMe_2 led to no reaction, as determined by ^1H NMR spectroscopy. This suggests that the (2,6-diisopropy-

Table 11. Selected Intramolecular Distances (Å) for 10

Ir1–Ir2	2.722(1)	Ir2–O	1.975(8)
Ir1–O	1.976(9)	Ir2–N	1.968(10)
Ir1–N	1.949(10)	Ir2–Cp2	1.786
Ir1–Cp1	1.780		

Table 12. Selected Intramolecular Angles (deg) for 10

Cp1–Ir1–O	136.1	O–Ir2–N	76.6(4)
Cp1–Ir1–N	146.0	Ir1–O–Ir2	87.1(3)
O–Ir1–N	77.0(4)	Ir1–N–Ir2	88.0(4)
Cp2–Ir2–O	135.1	Ir1–N–C21	134.0(9)
Cp2–Ir2–N	147.8	Ir2–N–C21	132.5(8)

Scheme 6

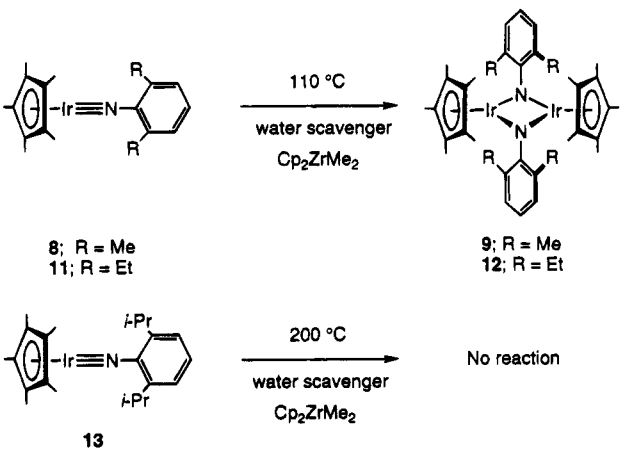

(34) Hunter, W. E.; Hrncir, D. C.; Bynum, R. V.; Penttila, R. A.; Atwood, J. L. *Organometallics* **1983**, *2*, 750.

(35) Complex **11** was prepared in 87% yield by a reaction analogous to that used to prepare **8**. The properties of this complex, including ^1H and $^{13}C\{^1H\}$ NMR resonances, relative solubility, and color, are very similar to those of the crystallographically characterized terminal arylimido complexes of iridium; see ref 13.

(36) Because this transformation required extended reaction time, some decomposition occurred, and therefore early reaction times were used to determine k_{obs}. Decreasing the concentration of **11** by a factor of 2 led to a halving of the rate of reaction but gave the same second-order rate constant.

(37) Attempts at solution molecular weight determinations were unsuccessful.

Scheme 7

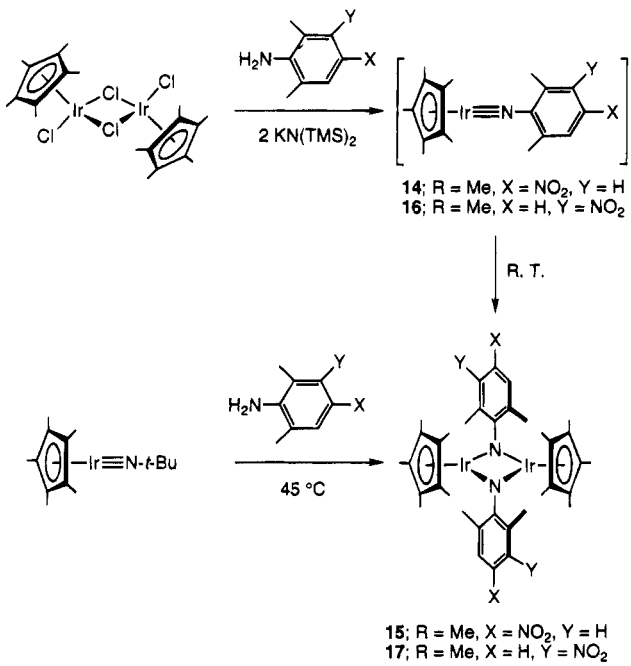

lphenyl)imido ligand is too sterically encumbered for dimerization to occur. We cannot determine whether this a kinetic or thermodynamic effect (i.e., the dimerization of **13** may be an endothermic process).

The fact that (dimethylphenyl)imido complex **8** dimerizes over 40 times faster than the corresponding diethyl complex **11** (and that the (2,6-diisopropylphenyl)imido complex **13** was not observed to dimerize under any conditions) may seem surprising in light of the small relative *A* value differences between a methyl and an ethyl group.[38] A better idea of the relative steric effects in this transition-metal system, in which four ethyl groups interact in the final product (2,6-diethylphenyl)-imido dimer **11** (and presumably in the transition state leading to this product), may be provided by comparison of the cone angles for PMe_3 (cone angle = 118°) and PEt_3 (cone angle = 132°).[39] Further, the size differential between PMe_3 and PEt_3 is demonstrated in the relative equilibrium constants of ligand dissociation reactions of these ligands from $Ni(PR_3)_4$ in which K_{eq} for R = Me is $<10^{-9}$ and K_{eq} for R = Et is 1.2×10^{-2}, indicating that dissociation of the larger triethylphosphine is significantly favored.

In addition to steric effects, electronic substitution on the aromatic ring of the imido ligand was expected to have an effect on the rate of dimerization. In order to test this hypothesis, we synthesized Cp*Ir≡N(2,6-dimethyl-4-nitrophenyl) (**14**). Treatment of $[Cp^*IrCl_2]_2$ with 1 equiv of 2,6-dimethyl-4-nitroaniline in THF with subsequent addition of potassium hexamethyldisilazane produced a complex which is best formulated as the monomer **14** on the basis of its ^1H NMR spectrum (*vide infra*) and its subsequently observed reactivity (Scheme 7). This complex could not be isolated, because it undergoes rapid dimerization upon concentration of the reaction mixture to produce Cp*Ir(μ-N(2,6-dimethyl-4-nitrophenyl))$_2$IrCp* (**15**). This complex was synthesized independently by the treatment of Cp*Ir≡N-*t*-Bu with 1 equiv of 2,6-dimethyl-4-nitroaniline in benzene at 45 °C for 24 h (Scheme 7). This complex was characterized by standard spectroscopic (*vide infra*) and analytical techniques.[37]

Because it is rapid, we cannot rule out the possibility that the presence of adventitious water catalyzes the dimerization of **14**. Addition of Cp_2ZrMe_2 to the reaction mixture resulted in decomposition. Therefore, it appears that the nitro group on the imido moiety is acting to increase the rate of the dimerization, but we cannot completely ensure that we are observing a simple thermal dimerization in this case. If the rapid dimerization is uncatalyzed, the *p*-NO_2 group is responsible for a surprisingly powerful substituent effect on the rate. We are not aware of any precedent for such an effect, and at present its physical source is unclear. The most likely explanation is that the strongly electron-withdrawing nitro group induces significant electronic polarization at the Ir=N linkage and that the rate is then enhanced by the resulting increased head-to-tail electrostatic interaction of the dimerizing (δ+)Ir=N(δ−) moieties. Another possible contribution to the rate might come from the possibility that for some reason the nitro group forces the imido ligand into a bent rather than a linear configuration. In such a complex, the lone pair at nitrogen would be more available for donation to another iridium center, which would now be electron deficient because of decreased N-to-Ir π donation. Testing these hypotheses requires the synthesis of analogous *p*-nitro-substituted arylimido systems that can be isolated and fully investigated structurally and kinetically.

Structures of the Imido Complexes. We were also interested in the structures of bridging imido complexes in the solid state and in solution. Through the synthesis of unsymmetrically substituted arylimido complexes, we obtained evidence for geometric isomers in solution. In analogy to the preparation of monomeric (2,6-dimethyl-4-nitrophenyl)imido complex **14**, treatment of $[Cp^*IrCl_2]_2$ with 2,6-dimethyl-3-nitroaniline followed by addition of potassium hexamethyldisilazane resulted in the formation of a complex which we formulate as monomeric imido complex Cp*Ir≡N(2,6-dimethyl-3-nitrophenyl) (**16**) on the basis of its ^1H NMR spectrum (*vide infra*) and its subsequent chemistry. Upon standing at room temperature, **16** was transformed into a mixture of two dimeric complexes with the empirical formulation Cp*Ir(μ-N(2,6-dimethyl-3-nitrophenyl))$_2$IrCp* (**17**). This mixture of complexes also was prepared in 69% yield by the treatment of Cp*Ir≡N-*t*-Bu with 2,6-dimethyl-3-nitroaniline (Scheme 7). ^1H and $^{13}C\{^1H\}$ NMR analysis (see Experimental Section) at room temperature indicates that the two isomers are present in a 60:40 ratio and that they do not interconvert upon heating to 80 °C.

We believe the 2,6-dimethyl-3-nitrophenyl imido complexes **17** are the syn and anti isomers shown in Scheme 8. Because the Ir_2N_2 cores of the (2,6-methyl-3-nitrophenyl)imido complexes **17** and other dimeric imido complexes are sterically crowded, rotation about the C—N linkage is a relatively slow process (Scheme 8). If **17** (except for fast Cp* rotation) is conformationally rigid in solution with the aryl rings of the imido ligands parallel to the planes of the Cp* ligand (similar to the solid state structure of (2,6-dimethylphenyl)imido com-

(38) The *A* value for methylcyclohexane is 1.70 kcal mol^{-1} and 1.75 kcal mol^{-1} for ethylcyclohexane. See: Hirsch, J. *Top. Stereochem.* **1967**, *1*, 199.
(39) Tolman, C. A. *Chem. Rev.* **1977**, *77*, 313.

Scheme 8

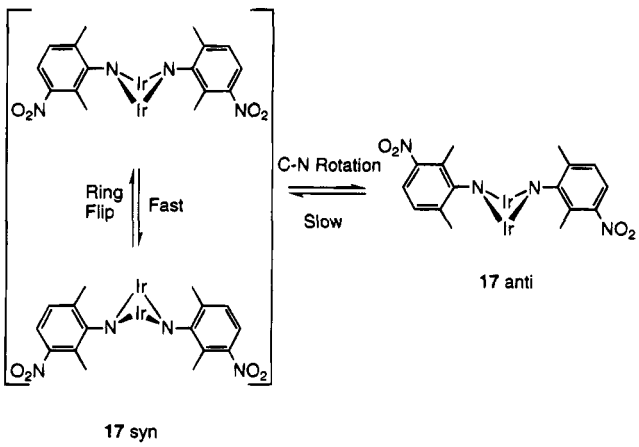

Scheme 9

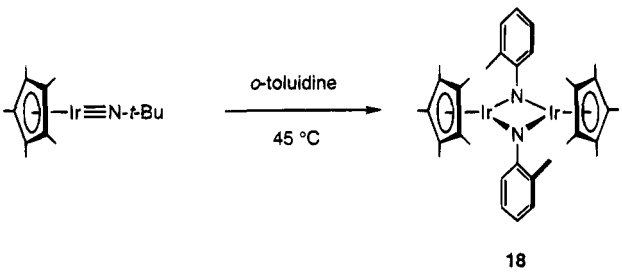

plex **9**, Figure 1), the observation of three isomers by ^{1}H NMR spectroscopy would be expected (Scheme 8). However, if ring inversion of the Ir_2N_2 core in these complexes is fast on the ^{1}H NMR time scale (no change in the ^{1}H NMR spectrum was observed upon cooling to −50 °C) and C—N bond rotation is slow, then two ismers with syn and anti orientations of the nitro groups would be expected, and this is consistent with what is observed.

In order to test further our hypothesis that these dimeric arylimido complexes have rigid aryl functionalities in solution, we synthesized a bridging imido complex with a (2-methylphenyl)imido ligand. Treatment of Cp*Ir≡N-*t*-Bu with 1 equiv of *o*-toluidine at 45 °C for 24 h resulted in the production of Cp*Ir(μ-N(2-methylphenyl))$_2$IrCp* (**18**) in 69% yield (Scheme 9). This complex displayed ^{1}H NMR resonances consistent with a single complex at room temperature. Upon cooling to −50 °C, however, in addition to these resonances, new resonances appeared consistent with the presence of 10% of an isomeric complex. These observations may be explained best by an isomerization process similar to that observed for asymmetric imido complex **17** (Scheme 10). We propose the (2-methylphenyl)imido dimer **18** should have a lower barrier to rotation about the C—N bond, because it is monosubstituted at the 2-position of the aromatic ring of the imido moiety, whereas complex **17** is disubstituted. The observed 10:1 ratio of resonances for **18** may be explained by the anti form of (2-methylphenyl)imido complex **18** dominating, which would minimize interactions between methyl groups on adjacent rings.

Correlation of ^{1}H NMR Spectral Data for Monomeric and Dimeric Imido Complexes. We have observed a trend in the chemical shift of the methyl resonance of the pentamethylcyclopentadienyl moiety in the iridium imido complexes in the ^{1}H NMR spectral

Scheme 10

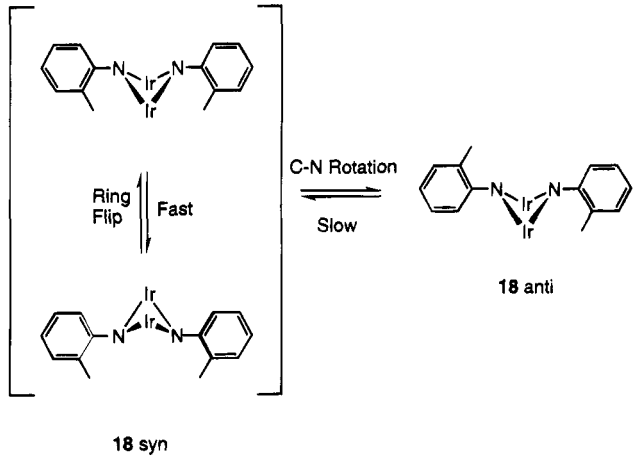

data. There appears to be a strong correlation between complexes possessing terminal imido ligands and chemical shift, and a similar correlation is observed for dimeric arylimido complexes but at a higher field (Figure 6). A possible explanation for this phenomenon is the following. If the aryl ring of the imido ligand is parallel to the plane of the pentamethylcyclopentadienyl ligand in the dimeric complexes in solution, then shielding of the methyl groups on the pentamethylcyclopentadienyl ligand from the anisotropy of the aryl groups may result (Figure 7).[40] In contrast, in the imido complexes with terminal imido functionality (linear Ir—N—C angle),[13] the aryl ring is perpendicular to the methyl groups and further away and this shielding would be expected to be diminished.[41] Whatever their physical basis, these chemical shift patterns provide additional support for our monomer and dimer structure assignments.

Summary

In contrast to our previous observations on iridium imido complexes that contain only terminally coordinated imido functionalities, we have synthesized dimeric analogues that contain sterically encumbered imido ligands in bridging conformations. These complexes undergo a variety of reactions, including atom transfer and reduction of an imido ligand by hydrogen. We also have shown that appropriately substituted terminal arylimido complexes undergo dimerization. This reaction is catalyzed by water but can proceed by thermal dimerization in the presence of the water-scavenger Cp_2ZrMe_2. The thermal dimerization was found to be sensitive to steric effects, and we have presented evidence that nitro substituents on the aromatic ring of such complexes also have an accelerating effect on the dimerization rate. Finally, we have obtained evidence for hindered rotation of the C—N bond in arylimido complexes. These results serve to broaden the scope of reactions known for iridium imido complexes and give evidence that some iridium imido complexes are thermodynamically favored in a dimeric as opposed to a monomeric form.

(40) A similar effect has been observed in another organometallic system and explained analogously, see: Dryden, N. H.; Legzdins, P.; Trotter, J.; Yee, V. C. *Organometallics* **1991**, *10*, 2857.

(41) Becker, E. D. *High Resolution NMR, Theory and Chemical Applications*, 2nd ed.; Academic Press: New York, 1980; p 74.

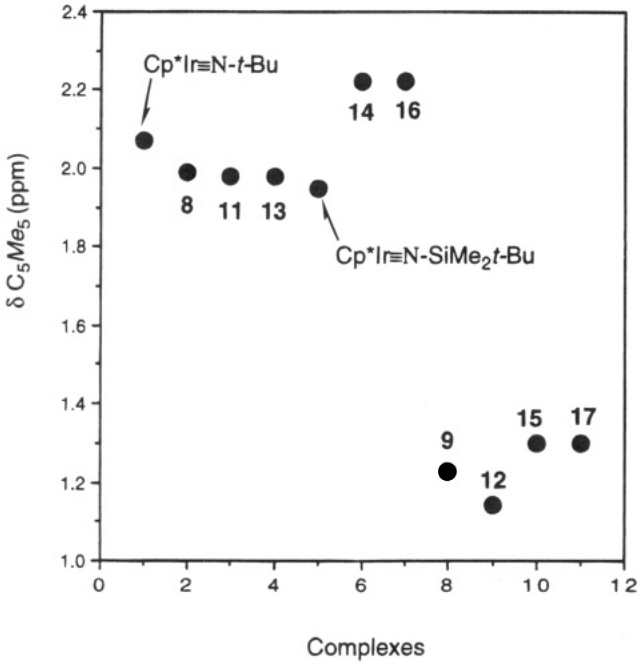

Figure 6. Correlation of ^{1}H NMR chemical shifts for the methyl groups on the pentamethylcyclopentadienyl ring of the monomeric and dimeric imido complexes Cp*Ir≡N-*t*-Bu, Cp*Ir≡NSiMe$_2$-*t*-Bu, **8**, **9**, and **11**−**17**. All data were collected in C_6D_6, except for complexes **14** and **16** which were obtained in THF-d_8.

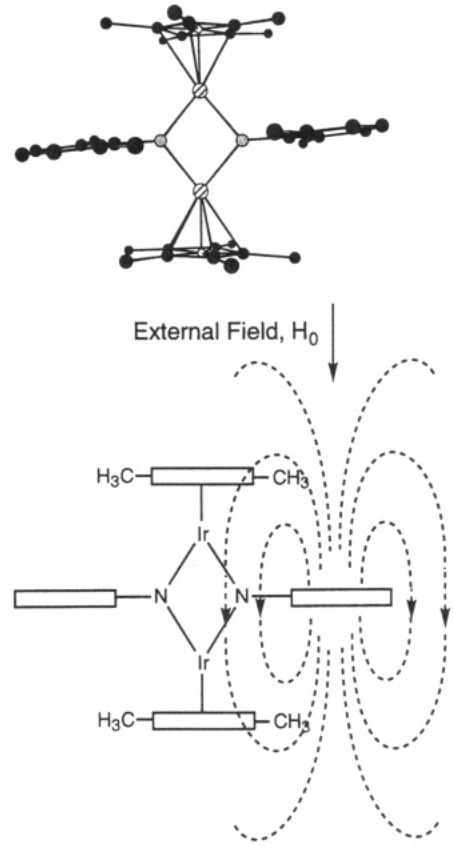

Figure 7. Chem3D representation of the crystal structure of complex **9** and an illustration of anisotropy of the aryl rings and the proximity of the methyl groups on the pentamethylcyclopentadienyl ligand.

Experimental Section

General Considerations. Unless otherwise noted, all reactions and manipulations were performed in dry glassware under a nitrogen atmosphere in a Vacuum Atmospheres 553-2 drybox equipped with an MO-40-2 Dri-train or by using standard Schlenk techniques on a high-vacuum line. All ^{1}H, ^{13}C{^{1}H}, and ^{31}P{^{1}H} NMR spectra were recorded on either a 300-MHz Fourier transform instrument constructed by Mr. Rudi Nunlist at the University of California, Berkeley NMR facility, Bruker AMX-300 or AMX-400 spectrometers, or a Bruker AM-400 spectrometer. Coupling constants are given in hertz. Infrared spectra were recorded on either a Nicolet 510 Fourier transform spectrometer or on a Mattson Galaxy Series FTIR 3000 spectrometer, and infrared absorptions are reported in cm^{-1}. Elemental analyses were performed at the University of California, Berkeley Microanalysis Facility, or at ONEIDA Analytical Laboratories, Whitesboro, NY. Mass spectral analyses were performed by the University of California, Berkeley Mass Spectrometry Laboratory, on AEI-MS12 and Kratos MS-50 instruments. Low-resolution (LR) and high-resolution (HR) mass spectral results are reported using the most abundant isotopes.

Benzene, diethyl ether, hexanes, pentane, THF, C_6D_6, toluene-d_8, THF-d_8, and toluene were distilled from sodium/benzophenone. Aniline, acetonitrile, acetonitrile-d_3, chloroform-d, and methylene-d_2 chloride were distilled from CaH_2. Cp*Ir≡N-*t*-Bu, Cp*Ir≡N(2,6-dimethylphenyl),[13] [Cp*IrCl$_2$]$_2$,[42] Cp$_2$ZrMe$_2$,[34] 2,6-dimethyl-3-nitroaniline, and 2,6-dimethyl-4-nitroaniline[43] were synthesized by literature procedures. Celite (diatomaceous earth) was dried overnight *in vacuo* at 200 °C. All other reagents were used as received from commercial suppliers. Reactions involving gases or low-boiling liquids were performed by condensation of a known pressure of gas from a bulk of known volume into the reaction mixture. In the case of hydrogen, the vessel was cooled to 77 K and was charged with a known volume of gas. All manipulations were performed at room temperature unless otherwise noted. The vessel referred to below as a "bomb" is a glass vessel sealed to a Kontes vacuum adapter.

Cp*Ir(μ-O)(μ-N-*t*-Bu)IrCp* (1). Into a 100-mL bomb was placed 234 mg Cp*Ir≡N-*t*-Bu (0.586 mmol) and 20 mL of THF. To this was added 18 μL of water under a purge of nitrogen. The reaction was stirred at room temperature for 7 days. The volatile materials were removed *in vacuo* for 1 h at 15 mTorr. The red solid was dissolved in pentane, filtered through a 2-cm × 2-cm pad of Celite, and the solvent was removed *in vacuo* to give 209 mg (0.562 mmol, 96%) of a red solid judged pure by ^{1}H NMR spectroscopy. An analytically pure sample was prepared by crystallization from a concentrated pentane solution at −40 °C: ^{1}H NMR (C_6D_6) δ 1.78 (s, 30 H, C_5Me_5), 1.65 (s, 9 H, CMe_3); ^{13}C{^{1}H} NMR (C_6D_6) δ 85.3 (s, C_5Me$_5$), 67.0 (s, CMe$_3$), 33.6 (s, CMe_3), 11.2 (s, C_5Me_5); IR (KBr) 2910 (s), 1639 (m), 1450 (m), 1379 (s), 1201 (s), 1029 (s), 622 (s), 551 (m) cm^{-1}; FAB MS *m/e* 740 (MH$^+$). Anal. Calcd for $C_{24}H_{39}Ir_2NO$: C, 38.85; H, 5.29; N, 1.89. Found: C, 38.49; H, 5.31; N, 1.93.

Cp*Ir(PPh$_2$Me)(μ-N-*t*-Bu)IrCp* (2). Into a 25-mL flask was added 100 mg of **1** (0.135 mmol), 10 mL of benzene, and 75 μL of PPh$_2$Me (0.400 mmol). The reaction mixture was stirred at room temperature for 7 days. The volatile materials were removed *in vacuo* for 2 h at 15 mTorr. The residue was extracted with a minimum of pentane and filtered through a 2-cm × 2-cm pad of Celite. The pentane solution was cooled quickly to −40 °C, and a white precipitate was formed. This compound was collected by filtration and identified as O=PPh$_2$-Me by ^{1}H NMR spectroscopy. The mother liquor was again cooled to −40 °C to give 65 mg (0.069 mmol, 51%) of **2** as red crystals: ^{1}H NMR (THF-d_8) δ 8.12 (m, 2 H, aryl), 7.40 (m, 3 H, aryl), 7.19 (d, J = 7.2 Hz, 2 H, aryl), 7.10 (m, 3 H, aryl), 1.67 (d, J = 1.5 Hz, 15 H, C_5Me_5Ir(P)), 1.66 (s, 15 H, C_5Me_5), 1.53 (d, J = 8.9 Hz, 3 H, P(Me)), 1.46 (s, 9 H, CMe_3); ^{13}C{^{1}H}

(42) Kang, J. W.; Moseley, K.; Maitlis, P. M. *J. Am. Chem. Soc.* **1969**, *91*, 5970.
(43) Bavin, P. M. G.; Scott, J. M. W. *Can. J. Chem.* **1958**, *36*, 1284.

NMR (THF-d_8) δ 143.1 (d, J = 41.2 Hz, aryl), 138.4 (d, J = 53.6 Hz, aryl), 137.8 (d, J = 12.5 Hz, aryl), 131.3 (d, J = 8.4 Hz, aryl), 129.9 (s, aryl), 128.0 (s, aryl), 127.8 (d, J = 8.7 Hz, aryl), 127.6 (d, J = 10.1 Hz, aryl), 91.7 (d, J = 4.9 Hz, C_5Me_5-Ir(P)), 81.8 (s, C_5Me_5), 69.0 (s, CMe_3), 33.5 (s, CMe_3), 19.4 (d, J = 38.1 Hz, P(Me)), 11.8 (s, C_5Me_5), 10.9 (s, C_5Me_5); $^{31}P\{^1H\}$ NMR (C_6D_6) δ 4.47 (s); IR (KBr) 2956 (s), 2912 (s), 1450 (m), 1188 (m), 1093 (m), 1028 (m), 881 (m), 746 (m), 698 (m), 511 (m) cm^{-1}; EI MS m/e 923 (M^+). Anal. Calcd for $C_{37}H_{52}Ir_2NP$: C, 47.98; H, 5.66; N, 1.51. Found: C, 47.76; H, 5.65; N, 1.57.

Crystal Structure Determination of Cp*Ir(PPh$_2$Me)(μ-N-*t*-Bu)IrCp* (2). Red crystals of **2** were obtained by slow diffusion of pentane into a toluene solution of **2** at room temperature. A single crystal was mounted in Paratone N hydrocarbon oil. The crystal was then transferred to an Enraf-Nonius CAD-4 diffractometer, centered in the beam, and cooled by a nitrogen-flow low-temperature apparatus. The final cell parameters and specific collection parameters are given in Table 1. The 6074 raw intensity data were converted to structure factor amplitudes and their esd's by correction for scan speed, background, and Lorentz and polarization effects. No correction for crystal decay was necessary. Space group $P\bar{1}$ was confirmed by refinement. The structure was solved by Patterson methods and refined *via* standard least-squares and Fourier techniques. Only the iridium and phosphorus atoms were refined with anisotropic thermal parameters. The final residues for **2** are given in Table 1.

The quantity minimized by the least-squares program was $\sum w(|F_o| - |F_c|)^2$, where w is the weight of a given observation. The p factor used to reduce the weight of intense reflections was set to 0.03 throughout the refinement. The analytical forms of the scattering factor tables for neutral atoms were used, and all scattering factors were corrected for both real and imaginary components of anomalous dispersion.

Cp*Ir(μ-NPh)$_2$IrCp* (3). A 25-mL flask was charged with 228 mg of Cp*Ir≡N-*t*-Bu (0.572 mmol) and 15 mL of benzene. To this solution was added 55.1 mg of aniline (0.592 mmol), and the solution was stirred at room temperature for 3 days. The volatile materials were removed *in vacuo* for 1 h at 15 mTorr. The resulting black solid was crystallized by dissolving in a minimum quantity of toluene and layering with pentane. The resulting solution was cooled to −40 °C to give 161 mg (0.383 mmol, 67%) of black crystals: ^1H NMR (C_6D_6) δ 7.32 (t, J = 6.8 Hz, 4 H, aryl), 7.17 (d, J = 6.8 Hz, 4 H, aryl), 6.98 (t, J = 6.8 Hz, 2 H, aryl), 1.46 (s, 30 H, C_5Me_5); $^{13}C\{^1H\}$ NMR (C_6D_6) δ 168.9 (s, aryl), 127.5 (s, aryl), 123.5 (s, aryl), 121.3 (s, aryl), 85.8 (s, C_5Me_5), 10.1 (s, C_5Me_5); IR (KBr) 3064 (m), 2912 (s), 1577 (s), 1473 (s), 1230 (vs), 1060 (m), 700 (s) cm^{-1}; FAB MS m/e (calcd) 835.2482, (found) 835.2472 (MH^+). Anal. Calcd for $C_{32}H_{40}Ir_2N_2$: C, 45.91; H, 4.82; N, 3.34. Found: C, 45.45; H, 4.88; N, 3.37.

Cp*Ir(μ-NPh)$_2$IrCp* (3) from Cp*Ir(μ-O)(μ-N-*t*-Bu)IrCp* (1). Into a 20-mL flask was placed 13.4 mg (0.018 mmol) of **1** and 2 mL of benzene. To the resulting solution was added 5.9 mg (0.060 mmol) of aniline. After 1 h the volatile materials were removed *in vacuo* for 1 h at 15 mTorr to give **3** which was shown by ^1H NMR spectroscopy to be identical to the complex produced by the reaction of Cp*Ir≡N-*t*-Bu and aniline.

Crystal Structure Determination of Cp*Ir(μ-NPh)$_2$IrCp* (3). Dark red crystals of **3** were obtained by slow diffusion of pentane into a toluene solution of **3** at room temperature. A single crystal was mounted as described for **2**. The final cell parameters and specific collection parameters are given in Table 1. The 2428 raw intensity data were converted to structure factor amplitudes and their esd's by correction for scan speed, background, and Lorentz and polarization effects. No correction for crystal decay was necessary. Space group *Pnnm* was confirmed by refinement. The structure was solved by Patterson methods and refined *via* standard least-squares and Fourier techniques. Only the iridium atoms were refined with anisotropic thermal parameters. The final residuals for **3** are given in Table 1. Minimization was carried out as for **2**.

PhN=PMe$_3$. This complex was prepared by a known method:[25] ^1H NMR ($CDCl_3$) δ 6.99 (t, J = 6.9 Hz, 2 H, *o*-aryl), 6.60 (d, J = 6.9 Hz, 2 H, *m*-aryl), 6.56), 6.56 (t, J = 6.9 Hz, 1 H, *p*-aryl), 1.49 (d, J = 12.4 Hz, 9 H, PMe_3); $^{13}C\{^1H\}$ NMR ($CDCl_3$) δ 151.5 (d, J = 4.4 Hz, aryl), 128.6 (d, J = 1.1 Hz, aryl), 122.0 (d, J = 18.4 Hz, aryl), 116.7 (d, J = 1.0 Hz, aryl), 15.7 (d, J = 67.1 Hz, PMe_3); $^{31}P\{^1H\}$ NMR ($CDCl_3$) δ 9.79 (s); EI MS m/e 167 (M^+).

Cp*Ir(PMe$_3$)(μ-NPh)IrCp* (4). To a 100-mL flask equipped with a vacuum adapter was added 536 mg (0.640 mmol) of **3** and 40 mL of benzene. To the resulting solution was added PMe_3 (3.84 mmol) by vacuum transfer (141 Torr/507 mL/298 K). The mixture was heated to 105 °C for 24 h. The volatile materials were removed *in vacuo* for 2 h at 15 mTorr. The resulting solid was recrystallized by dissolving in a minimum amount of toluene, layering with hexamethyldisiloxane, and cooling to −40 °C. This produced 125 mg (0.150 mmol, 24%) of **4** as black crystals which were isolated by filtration: ^1H NMR (C_6D_6) δ 7.83 (d, J = 8.3 Hz, 2 H, aryl), 7.23 (t, J = 8.3 Hz, 2 H, aryl), 6.88 (t, J = 8.3 Hz, 1 H, aryl), 2.04 (d, J = 1.8 Hz, 15 H, C_5Me_5Ir(P)), 1.85 (s, 15 H, C_5Me_5), 1.09 (d, J = 9.4 Hz, 9 H, PMe_3); $^{13}C\{^1H\}$ NMR (C_6D_6) δ 165.3 (s, aryl), 129.0 (s, aryl), 124.0 (s, aryl), 119.0 (s, aryl), 90.6 (d, J = 4.2 Hz, C_5Me_5Ir(P)), 81.8 (s, C_5Me_5), 20.6 (d, J = 35.2 Hz, PMe_3), 12.1 (s, C_5Me_5), 11.3 (s, C_5Me_5); $^{31}P\{^1H\}$ NMR (C_6D_6) δ 38.0 (s); IR (KBr) 2900 (s), 1577 (m), 1463 (s), 1272 (vs), 1145 (m), 946 (m) cm^{-1}; FAB MS m/e 820 (MH^+). Anal. Calcd for $C_{29}H_{44}Ir_2NP$: C, 42.37; H, 5.40; N, 1.70. Found: C, 41.95; H, 5.30; N, 1.73.

Cp*Ir(PMe$_3$)(μ-NPh)$_2$IrCp* (5). This complex was observed as an intermediate in the conversion of **3** into **4** by NMR spectroscopy: ^1H NMR (C_6D_6) δ 7.21 (dd, J = 7.0 Hz, J = 8.6 Hz, 4 H, aryl), 6.80 (d, J = 7.0 Hz, 4 H, aryl), 6.67 (t, J = 7.0 Hz, 2 H, aryl), 1.63 (s, 15 H, C_5Me_5), 1.34 (d, J = 1.8 Hz, 15 H, C_5Me_5Ir(P)), 1.25 (d, J = 10.2 Hz, 9 H, PMe_3); $^{31}P\{^1H\}$ NMR (C_6D_6) δ −34.6 (s).

Cp*Ir(μ-NH(*o*-C$_6$H$_5$))(μ-H)$_2$IrCp* (7) to a 50-mL bomb was added 479 mg (0.575 mmol) of **3** and 20 mL of benzene. The resulting solution was frozen (77 K), the headspace in the bomb was evacuated, and the bomb was charged with 2 atm of H_2 (400 Torr/77 K/ 20 mL). The solution was heated to 70 °C for 2 days. The volatile materials were removed *in vacuo* for 2 h at 15 mTorr. The purple solid was dissolved in a minimum quantity of toluene layered with pentane and cooled to −40 °C. This provided 235 mg (0.322 mmol) of **6** as purple crystals: ^1H NMR (THF-d_8) δ 10.12 (s, 1 H, N*H*), 8.05 (d, J = 7.2 Hz, 1 H, aryl), 7.27 (d, J = 7.2 Hz, 1 H, aryl), 6.56 (t, J = 7.2 Hz, aryl), 6.34 (t, J = 7.2 Hz, 1 H, aryl), 2.15 (s, 15 H, C_5Me_5), 2.11 (s, 15 H, C_5Me_5), =16.80 (s, 2 H, Ir*H*); $^{13}C\{^1H\}$ NMR (THF-d_8) δ 170.3 (s, aryl), 147.6 (s, aryl), 142.4 (s, aryl), 121.9 (s, aryl), 113.6 (s, aryl), 111.8 (s, aryl), 91.3 (s, C_5Me_5), 87.2 (s, C_5Me_5), 11.0 (s, C_5Me_5), 10.6 (s, C_5Me_5); IR (KBr) 2912 (S), 1429 (m), 1375 (m), 1322 (s), 1029 (s), 719 (m) cm^{-1}; FAB MS m/e (calcd) 748.2245, (found) 748.2240 (MH^+). Anal. Calcd for $C_{26}H_{37}Ir_2N$: C, 41.75; H, 4.99; N, 1.87. Found: C, 41.26; H, 4.96; N, 1.97.

Crystal Structure Determination of Cp*Ir(μ-NH(*o*-C$_6$H$_4$))(μ-H)$_2$IrCp* (7). A purple crystal of **7** was obtained by slow diffusion of pentane into a concentrated toluene solution. Fragments cleaved from this crystal were mounted as described for **2**. Crystal quality reciprocal space, automatic peak search, and indexing procedures yielded a triclinic reduced primitive cell. Inspection of the Niggli values and specific data collection parameters for the data set are given in Table 1.

The 8444 raw intensity data were converted to structure factor amplitudes and their esd's by correction for scan speed, background, and Lorentz and polarization effects. No correction for crystal decay was necessary. Inspection of the azimuthal scan data showed a variation I_{min}/I_{max} = 0.50 for

the average curve. Initially, an empirical correction based on the observed variation was applied to the data. Following solution and refinement of the structure the presence of symmetrical peaks in the difference Fourier map around the iridium atoms suggested that this correction had been insufficient. Therefore an empirical correction was made to the data on the basis of the combined differences of F_o and F_c following refinement of all atoms with isotropic thermal parameters ($T_{max} = 1.29$, $T_{min} = 0.84$).[44] Redundant data were averaged to give 4351 unique data ($R_I = 2.4\%$). The centric space group was confirmed by the successful solution and refinement of the structure.

The structure was solved by Patterson methods and refined *via* standard least-squares and Fourier techniques. In a difference Fourier map calculated following the refinement of all non-hydrogen atoms with anisotropic thermal parameters, peaks were found corresponding to the positions of most of the hydrogen atoms in the approximately 1.2 times the B_{eq} of the atoms to which they were attached. They were included in structure factor calculation, but not refined. In a subsequent difference Fourier map, peaks were discovered which corresponded to reasonable positions for the hydride and amido hydrogen atoms. These three were included in structure factor calculations, and their positional and isotropic thermal parameters were refined. In the final cycles of least-squares four data with abnormally large weighted difference, values were given zero weight. The final residuals for **7** are given in Table 1. In the final cycles of refinement a secondary extinction parameter was included (maximum correction = 6% on F).

Minimization was carried out as for **2**. Inspection of the residuals ordered in ranges of $(\sin\theta)/\lambda$, $|F_o|$, and parity and value of the individual indexes showed no unusual features or trends. The largest peak in the final difference Fourier map had an electron density of 0.82 e/Å^3, and the lowest excursion −0.25 e/Å^3. All large peaks were located near iridium atoms.

Cp*Ir(μ-N(2,6-dimethylphenyl))$_2$IrCp* (9). To a 50-mL flask was added 146 mg (0.327 mmol) of Cp*Ir≡N(2,6-dimethylphenyl) (**8**) and 15 mL of benzene. This solution was heated to 45 °C for 2 days. The solvent was removed *in vacuo* for 2 h at 15 mTorr. The resulting red solid was crystallized from toluene layered with pentane at −40 °C. This gave 135 mg (0.302 mmol, 92%) of **9** as purple crystals: ^{1}H NMR (C_6D_6) δ 7.34 (d, J = 7.4 Hz, 4 H, $Me_2C_6H_3N$), 7.01 (t, J = 7.4 Hz, 2 H, $Me_2C_6H_3N$), 2.49 (s, 12 H, $Me_2C_6H_3N$), 1.23 (s, 30 H, C_5Me_5); ^{13}C{^{1}H} NMR (C_6D_6) δ 161.0 (s, aryl), 131.1 (s, aryl), 127.8 (s, aryl), 121.4 (s, aryl), 83.4 (s, C_5Me_5), 19.5 (s, $Me_2C_6H_3N$), 8.87 (s, C_5Me_5); IR (KBr) 2977 (m), 2906 (s), 1452 (m), 1224 (s), 1091 (m), 1031 (m), 754 (w) cm^{-1}; FAB MS *m/e* 892 (MH$^+$). Anal. Calcd for $C_{36}H_{48}Ir_2N_2$: C, 48.41; H, 5.42; N, 3.14. Found: C, 48.33; H, 5.20; N, 3.11.

Crystal Structure Determination of Cp*Ir(μ-N(2,6-dimethylphenyl))$_2$IrCp* (9). Purple crystals of **9** were obtained by slow diffusion of pentane into a toluene solution at room temperature. A single crystal was mounted as described for **2**. The final cell parameters and specific collection parameters are given in Table 1. The 3169 raw intensity data were converted to structure factor amplitudes and their esd's by correction for scan speed, background, and Lorentz and polarization effects. No correction for crystal decay was necessary. Space group $C2/c$ was confirmed by refinement. The structure was solved by Patterson methods and refined *via* standard least-squares and Fourier techniques. Only the iridium atom was refined with anisotropic thermal parameters. The final residuals for **9** are given in Table 1. Minimization was carried out as for **2**.

Improved Preparation of Cp*Ir(μ-O)$_2$IrCp*. $AgNO_3$ (665 mg, 3.91 mmol) was dissolved in H_2O (20 mL) and treated with NaOH (313 mg, 7.82 mmol) dissolved in H_2O (10 mL). After 1 min of stirring, the solid materials in the reaction mixture were allowed to settle and the brown precipitate (AgO) was isolated by cannula filtration. The precipitate was washed with H_2O (3 × 40 mL). To this precipitate was added $[Cp^*IrCl_2]_2$ (588 mg, 0.738 mmol) and 50 mL of H_2O. The resulting slurry was stirred for 1 h at room temperature, after which time the white precipitate that had formed (AgCl) was filtered off using Celite. The filtrate was taken to dryness first using a rotary evaporator and then high vacuum. The resulting brown solid was suspended in benzene (50 mL) and lyophilized overnight. The resulting red powder was collected; it was established to be $[Cp^*IrO]_2$ by comparison of its ^{1}H and ^{13}C{^{1}H} NMR spectra with those of an authentic sample. Yield: 330 mg (0.480 mmol, 65% from $[Cp^*IrCl_2]_2$).

Cp*Ir(μ-O)(μ-N(2,6-dimethylphenyl))IrCp* (10). To a 20-mL flask was added 145 mg (0.213 mmol) of Cp*Ir(μ-O)$_2$IrCp* and 10 mL of benzene. To this was added 21 mg (0.173 mmol) of aniline dissolved in 5 mL of benzene. The solution was stirred for 10 min. The volatile materials were removed *in vacuo* for 2 h at 15 mTorr. The resulting red solid was recrystallized from a minimum amount of toluene layered with pentane and cooled to −40 °C. This gave 47 mg (0.060 mmol, 28%) of **10** as red crystals: ^{1}H NMR (C_6D_6) δ 7.17 (d, J = 7.5 Hz, 2 H, $Me_2C_6H_3N$), 6.95 (t, J = 7.5 Hz, 1 H, $Me_2C_6H_3N$), 2.31 (s, 6 H, $Me_2C_6H_3N$), 1.60 (s, 15 H, C_5Me_5); ^{13}C{^{1}H} NMR (C_6D_6) δ 162.5 (s, aryl), 127.2 (s, aryl), 126.4 (s, aryl), 121.7 (s, aryl), 84.7 (s, C_5Me_5), 19.0 (s, $Me_2C_6H_3N$), 10.1 (s, C_5Me_5); IR (C_6H_6) 2908 (s), 1457 (m), 1387 (m), 1236 (m), 1024 (m), 759 (w) cm^{-1}; FAB MS *m/e* 790 (MH$^+$). Anal. Calcd for $C_{28}H_{39}Ir_2NO$: C, 42.57; H, 4.98; N, 1.77. Found: C, 42.55; H, 4.96; N, 1.73.

Crystal Structure Determination of Cp*Ir(μ-O)(μ-N(2,6-dimethylphenyl))IrCp* (10). Red crystals of **10** were obtained by slow diffusion of pentane into a toluene solution at room temperature. A single crystal was mounted as described for **2**. The final cell parameters and specific collection parameters are given in Table 1. The 3791 raw intensity data were converted to structure factor amplitudes and their esd's by correction for scan speed, background, and Lorentz and polarization effects. Maximum correction for crystal decay was 1.3% on F. The space group $P2_1/n$ was confirmed by refinement. The structure was solved by Patterson methods and refined *via* standard least-squares and Fourier techniques. Only the iridium atom was refined with anisotropic thermal parameters. The final residuals for **10** are given in Table 1. Minimization was carried out as for **3**.

Cp*Ir≡N(2,6-diethylphenyl) (11). Into a 100-mL flask was placed 1.13 g (1.42 mmol) of $[Cp^*IrCl_2]_2$ and 902 mg (5.82 mmol) of LiNH(2,6-diethylphenyl). This mixture was cooled to 77 K and 50 mL of THF was added *via* vacuum transfer. The mixture was then warmed to 0 °C and stirred for 1 h. The volatile materials were removed at 0 °C for 2 h at 10 mTorr. The resulting yellow solid was extracted with a minimum amount of toluene and filtered through a 2-cm × 2-cm pad of Celite. This toluene solution was layered with pentane and cooled to −40 °C. This gave 802 mg (2.47 mmol, 87%) of **11** as yellow needles: ^{1}H NMR (C_6D_6) δ 7.10 (t, J = 7.5 Hz, 1 H, $(MeCH_2)_2C_6H_3N$), 6.89 (d, J = 7.5 Hz, 2 H, $(MeCH_2)_2C_6H_3N$), 2.91 (q, J = 7.6 Hz, 4 H, $(MeCH_2)_2C_6H_3N$), 1.98 (s, 15 H, C_5Me_5), 1.36 (t, J = 7.6 Hz, 6 H, $(MeCH_2)_2C_6H_3N$); ^{13}C{^{1}H} NMR (C_6D_6) δ 150.1 (s, aryl), 139.5 (s, aryl), 126.2 (s, aryl), 123.6 (s, aryl), 84.9 (s, C_5Me_5), 26.0 (s, CH_2), 14.1 (s, CH_3), 11.3 (s, C_5Me_5); IR (KBr) 2966 (s), 2921 (s), 2863 (s), 1438 (s), 1344 (s), 802 (m), 769 (m) cm^{-1}. Anal Calcd for $C_{20}H_{28}IrN$: C, 50.61; H, 5.95; N, 2.95. Found: C, 50.51; H, 5.95; N, 2.96.

Cp*Ir(μ-N(2,6-diethylphenyl))$_2$IrCp* (12). Into a 50-mL bomb was placed 100 mg (0.251 mmol) of Cp*Ir≡N-*t*-Bu and 41 mg (0.275 mmol) of 2,6-diethylaniline. To this was added 15 mL of toluene which was degassed but not dried. The resulting solution was heated to 75 °C for 2 days. The volatile materials were removed *in vacuo* for 2 h at 15 mTorr. The purple solid was then dissolved in a minimum amount of pentane and cooled to −40 °C. This gave 78.5 mg (0.166 mmol, 66%) of **12** as purple crystals: ^{1}H NMR (C_6D_6) δ 7.42 (d, J =

(44) Walker, N.; Stuart, D. *Acta Crystallogr.* **1983**, *A39*, 159.

7.5 Hz, 2 H, $(MeCH_2)_2C_6H_3N$), 7.20 (t, J = 7.5 Hz, 1 H, $(MeCH_2)_2C_6H_3N$), 2.93 (q, J = 7.6 Hz, 4 H, $(MeCH_2)_2C_6H_3N$), 1.50 (t, J = 7.6 Hz, 6 H, $(MeCH_2)_2C_6H_3N$), 1.14 (s, 15 H, C_5Me_5); $^{13}C\{^1H\}$ NMR (C_6D_6) δ 159.4 (s, aryl), 135.4 (s, aryl), 123.4 (s, aryl), 121.8 (s, aryl), 83.9 (s, C_5Me_5), 24.0 (s, CH_2), 13.1 (s, CH_3), 8.8 (s, C_5Me_5); IR (KBr) 2954 (s), 2908 (s), 1429 (s), 1243 (s), 1031 (s), 777 (m) cm^{-1}; FAB MS *m/e* 947 (MH^+). Anal. Calcd for $C_{40}H_{56}Ir_2N_2$: C, 50.61; H, 5.95; N, 2.95. Found: C, 50.94; H, 5.98; N, 2.83.

Cp*Ir≡N(2,6-dimethyl-4-nitrophenyl) (14). To a 20-mL flask was added 8.6 mg (0.011 mmol) of $[Cp^*IrCl_2]_2$, 3.6 mg (0.022 mmol) of 2,6-dimethyl-4-nitroaniline, and 1 mL of CH_2Cl_2. The resulting solution was stirred for 1 h. The solvent was removed *in vacuo*, and the resulting yellow powder was suspended in 0.5 mL of THF-d_8 and cooled to −78 °C. To this solution was added 8.9 mg (0.044 mmol) of potassium hexamethyldisilazane dissolved in 0.3 mL THF-d_8 by syringe. The solution was warmed to room temperature and examined by ^1H NMR spectroscopy. The complex produced was found to be unstable upon concentration of the reaction mixture and could not be isolated: ^1H NMR (THF-d_8) δ 7.73 (s, 2 H, $C_6H_2(Me)_2NO_2$), 2.23 (s, 15 H, C_5Me_5), 2.16 (s, 6 H, $C_6H_2(Me)_2NO_2$).

Cp*Ir(μ-N(2,6-dimethyl-4-nitrophenyl))$_2$IrCp* (15). To a 25-mL bomb was added 61.9 mg (0.155 mmol) of Cp*Ir≡N-*t*-Bu, 26.3 mg (0.158 mmol) of 2,6-dimethyl-4-nitroaniline, and 2 mL of benzene. The resulting solution was heated at 45 °C for 24 h. The black crystals that formed during heating were isolated by filtration, and washed with 5 mL of benzene. The excess solvent was removed from the crystals *in vacuo* for 2 h at 15 mTorr, affording 36 mg of **15**. The mother liquor was layered with pentane and after 24 h 20 mg of **15** was isolated. The total amount of product isolated as black crystals was 56 mg (0.057 mmol, 73%): ^1H NMR (CD_2Cl_2) δ 8.06 (s, 4 H, $C_6H_2(Me)_2NO_2$), 2.34 (s, 12 H, $C_6H_2(Me)_2NO_2$), 1.27 (s, 30 H, C_5Me_5); $^{13}C\{^1H\}$ NMR (CD_2Cl_2) 140.9 (s, aryl), 133.2 (s, aryl), 124.7 (s, aryl), 123.3 (s, aryl), 83.9 (s, C_5Me_5), 19.4 (s, $C_6H_2(Me)_2NO_2$), 9.0 (s, C_5Me_5); IR (KBr) 2910 (m), 1575 (m), 1494 (m), 1311 (s), 1257 (s), 1234 (s), 1091 (s), 943 (m), 763 (w) cm^{-1}. Anal. Calcd for $C_{36}H_{46}Ir_2N_4O_4$: C, 43.98; H, 4.72; N, 5.70. Found: C, 44.41; H, 4.62; N, 5.52.

Cp*Ir≡N(2,6-dimethyl-3-nitrophenyl) (16). This complex was prepared by a method analogous to that used to produce **14** and was found to be similarly unstable: ^1H NMR (THF-d_8) δ 7.47 (d, J = 8.4 Hz, 2 H, $C_6H_2(Me)_2NO_2$), 6.93 (d, J = 8.4 Hz, 2 H, $C_6H_2(Me)_2NO_2$), 2.28 (s, 3 H, $C_6H_2(Me)_2NO_2$), 2.23 (s, 30 H, C_5Me_5), 2.15 (s, 3 H, $C_6H_2(Me)_2NO_2$).

Cp*Ir(μ-N(2,6-dimethyl-3-nitrophenyl))$_2$IrCp* (17) (syn and anti). Into a 25-mL bomb wsa added 98.8 mg (0.248 mmol) of Cp*Ir≡N-*t*-Bu, 42 mg (0.253 mmol) of 2,6-dimethyl-3-nitroaniline, and 2 mL of benzene. The resulting solution was heated at 45 °C for 24 h. The black crystals formed during heating were isolated by filtration and washed with 5 mL of benzene. The excess benzene was removed from the crystals *in vacuo*, and this afforded 75.6 mg of **17**. The mother liquor was layered with pentane, and after 24 h, 30 mg of **17** was isolated. The total amount of **17** isolated as black crystals was 106 mg (0.108 mmol, 87%): ^1H NMR (CD_2Cl_2) δ 7.33 (d, J = 8.3 Hz, 2 H, $C_6H_2(Me)_2NO_2$), 7.33 (d, J = 8.3 Hz, 2 H, $C_6H_2(Me)_2NO_2$), 7.20 (d, J = 8.3 Hz, 2 H, $C_6H_2(Me)_2NO_2$), 7.18 (d, J = 8.3 Hz, 2 H, $C_6H_2(Me)_2NO_2$), 2.54 (s, 6 H, $C_6H_2(Me)_2NO_2$), 2.48 (s, 6 H, $C_6H_2(Me)_2NO_2$), 2.36 (s, 6 H, $C_6H_2(Me)_2NO_2$), 2.28 (s, 6 H, $C_6H_2(Me)_2NO_2$), 1.27 (s, 30 H, C_5Me_5), 1.26 (s, 30 H, C_5Me_5); $^{13}C\{^1H\}$ NMR (CD_2Cl_2) 162.2 (s, aryl), 162.1 (s, aryl), 149.9 (s, aryl), 149.7 (s, aryl), 138.4 (s, aryl), 138.0 (s, aryl), 127.1 (s, aryl), 126.8 (s, aryl), 126.0 (s, aryl), 125.5 (s, aryl), 116.5 (s, aryl), 116.4 (s, aryl), 84.1 (s, C_5Me_5), 84.0 (s, C_5Me_5), 20.2 (s, $C_6H_2(Me)_2NO_2$), 20.1 (s, $C_6H_2(Me)_2NO_2$), 15.2 (s, $C_6H_2(Me)_2NO_2$), 15.0 (s, $C_6H_2(Me)_2NO_2$), 9.1 (s, C_5Me_5), 9.0 (s, C_5Me_5); IR (KBr) 2912 (m), 1510 (s), 1340 (s), 1247 (s), 1031 (m), 827 (m), 813 (m), 744 (m) cm^{-1}. Anal. Calcd for $C_{36}H_{46}Ir_2N_4O_4$: C, 43.98; H, 4.72; N, 5.70. Found: C, 43.79; H, 4.54; N, 5.60.

Cp*Ir(μ-N(2-methylphenyl))$_2$IrCp* (18). To a 100-mL bomb was added 94.5 mg (0.237 mmol) of Cp*Ir≡N-*t*-Bu, 30.4 mg (0.284 mmol) of *o*-toluidine, and 10 mL of pentane. The resulting solution was heated at 45 °C for 24 h, during which time deep red crystals formed and were isolated by filtration, affording 49 mg of **18**. The mother liquor was cooled to −40 °C and produced a second crop of deep red crystals, which were isolated, affording 21 mg of **18** totaling 70 mg (0.081 mmol, 69%): ^1H NMR (CD_2Cl_2) δ 7.15 (t, J = 7.3 Hz, 2 H, MeC_6H_4), 7.05 (d, J = 7.3 Hz, 2 H, MeC_6H_4), 6.85 (d, J = 7.3 Hz, 2 H, MeC_6H_4), 6.78 (t, J = 7.3 Hz, 2 H, MeC_6H_4), 1.88 (s, 6 H, MeC_6H_4), 1.50 (s, 30 H, C_5Me_5); $^{13}C\{^1H\}$ NMR (CD_2Cl_2) δ 166.3 (s, MeC_6H_4), 130.0 (s, MeC_6H_4), 128.6 (s, MeC_6H_4), 125.2 (s, MeC_6H_4), 124.1 (s, MeC_6H_4), 120.9 (s, MeC_6H_4), 86.0 (s, C_5Me_5), 18.2 (s, MeC_6H_4), 10.0 (s, C_5Me_5); IR (KBr) 2981 (m), 2908 (m), 1587 (m), 1467 (m), 1234 (s), 1031 (m), 879 (w), 727 (m) cm^{-1}; FAB MS *m/e* 865 (MH^+). Anal. Calcd for $C_{34}H_{44}Ir_2N_2$: C, 47.20; H, 5.13; N, 3.24. Found: C, 47.12; H, 5.03; N, 3.02.

Kinetics. All kinetic experiments were monitored by ^1H NMR spectroscopy in THF-d_8 at 20 °C using Bruker AMX-400 or -300 MHz NMR spectrometers. Standard solutions of compounds **8** and **11** were prepared in the drybox using volumetric pipets and were stored in a −40 °C freezer. Individual samples were prepared by transferring this solution onto a weighed sample of Cp_2ZrMe_2 in a 10-mL vial and after dissolution into a new dry 8-in. Wilmad NMR tube. An internal standard (*p*-dimethoxybenzene) dissolved in THF-d_8 to produce a standard solution was then added by syringe. A metal Cajon adapter connected to a Kontes high-vacuum stopcock was attached to the tube, and the solution was frozen (77 K) and flame-sealed. The sample was placed into the NMR spectrometer, and the initial concentrations were measured. The NMR tube was removed and placed in a constant temperature bath at 110 or 200 °C. The sample was removed at intervals, cooled rapidly to 0 °C, and then monitored by ^1H NMR spectroscopy after warming to room temperature.

Reactions were monitored by observing the appearance of the resonance for the methylene ligand of **11** or the pentamethylcyclopentadienyl ligand of **8**. Plots of (concentration)$^{-1}$ versus time were plotted using the KaleidaGraph program.

Acknowledgment. We are grateful for support of this work from the National Science Foundation (Grant No. CHE-9113261). We also acknowledge a gift of iridium chloride from the Johnson-Matthey Aesar/Alfa metal loan program. We would like to thank Dr. F. J. Hollander for determination of the crystal structures of complexes **2**, **3**, **7**, **9**, and **10**, and we would like to thank Dr. Keith A. Woerpel and Dr. Patrick J. Walsh for many insightful discussions.

Supplementary Material Available: Tables of X-ray diffraction data (positional and anisotropic thermal parameters and full intramolecular distances and angles) for **2**, **3**, **7**, **9**, and **10** (13 pages). This material is provided with the archival edition of the journal, available in many libraries. Alternatively, ordering information is given on any current masthead page.

OM940616V